Mechanisms of mesoscopic patterning in evaporated polymer films deposited on tilted and vertical substrates

ED. BORMASHENKO*, R. POGREB, O. STANEVSKY, YE. BORMASHENKO, T. STEIN, R. COHEN, SH. REIS
The College of Judea and Samaria, The Laboratory of Polymer Materials, Ariel, 44837, Israel
E-mail: edward@ycariel.yosh.ac.il

O. V. GENDELMAN
Technion, Technion City 32000, Faculty of Mechanical Engineering, Haifa, Israel

Published online: 12 January 2006

Mesoscopic self-organization in evaporated polymer solutions was investigated. The structure of dried films was studied with optical and SEM microscopy. Formation of mesoscopic cells was studied *in situ* with a shadowgraph technique. Intensive migration of the vapor bubbles is an important factor in the formation of mesoscopic cells. A mechanism of mesoscopic network formation, based on the mass transport instability in evaporated film, was proposed. The impact of the solvent is discussed.

1. Introduction

Evaporation-induced mesoscopic patterning in organic and non-organic liquids was under intensive investigation recently [1–5]. Very different regular patterns, including periodic structures and spirals, were observed [3–8]. Mesoscopic patterning attracted particular interest for two main reasons: firstly, understanding its mechanisms is important for enhancing polymer coatings; secondly, new applications of mesoscopic structures were proposed. Among them, M. Shimomura reported use of mesoscopically patterned polymer films as novel biofunctional interfaces intended for cell growth [9].

Much theoretical effort was devoted to understanding the mechanisms responsible for mesoscopic patterning. Two main approaches could be recognized: the first treats mesoscopic structuring as a process of cracking under solvent evaporation [10, 11]; and the second approach relates mesoscopic self-assembling to various kinds of surface instabilities such as Marangoni surface tension instability [3, 4, 12–18]. It has to be emphasized that describing physical processes occurring in evaporating films turns out to be very challenging, since couplings between the microstructure and hydrodynamic flow are highly nonlinear [19, 20]. Within recent years, there were several attempts to work out the mathematical model describing a flow of evaporated liquid layers, considering strong non-linearities inherent to such flows [21–27]. The impact of the Soret effect on the mesoscopic patterning was studied as well [22]. At the same time, a comprehensive understanding of the mesoscopic structuring occurring under the evaporation of polymer liquids has still not been achieved.

De Gennes recently has shown that mesoscopic self-organization may be due to some non-Marangoni kind of instability [12]. He has shown that in an evaporating film, a convective instabilities are due to the concentration effects (when the surface tension of polymer σ_p is higher than the surface tension of the solvent σ_s): a region of upward flow ("plume") of solvent-rich fluid induces a local depression in surface tension, and the surface forces tend to strengthen the plume. His calculations led to the conclusion that when $\sigma_p > \sigma_s$, this kind of instability should dominate over the classic Bénard-Marangoni instabilities. However, De Gennes already indicated that this model does not explain high roughness of PS/acetone films (when $\sigma_p < \sigma_s$) and low roughness of PS/toluene films, when $(\sigma_p > \sigma_s)$ [13]. Thus De Gennes supposed that these phenomena are due to "crust" effects: a polymer-rich "crust" builds up near the free surface: when it dries out, it is under tension and should rupture—creating mesoscopic crack patterns, as reported by different groups

*Author to whom all correspondence should be addressed.
0022-2461
DOI: 10.1007/s10853-005-2376-y

[3, 4, 6, 7]. Our experimental work will show that the real situation in the evaporated film is more complicated: mesoscopic patterns are substantially due to the migration of vapor bubbles, formed under the evaporation of the solvent.

Physical properties (including their viscosities and transport properties) of organic solvents used in our investigation were studied thoroughly experimentally and reported by different groups [28–30].

2. Experimental

Three kinds of polymers: polystyrene (PS) 143 E (supplied by BASF), polycarbonate (PC) Lexan 141 (supplied by GE Plastics) and polymethylmethacrylate (PMMA) Acrylex CM 205 (supplied by Chi Mei Corp), were dissolved in two groups of organic solvents: chlorinated (dichloromethane CH_2Cl_2 and chloroform $CHCl_3$) and aromatic: (toluene and xylenes). All solvents were supplied by Karlo Erba Reagenti, the concentration of the solution was 5% wt for all kinds of polymers and solvents. Two types of substrates (quartz glass and polypropylene (PP)) were coated with different experimental techniques: fast dip-coating and deposition on the tilted substrates (see Fig. 1A and B). Substrates were cleaned thoroughly with acetone and ethyl alcohol and rinsed with a large amount of distilled water.

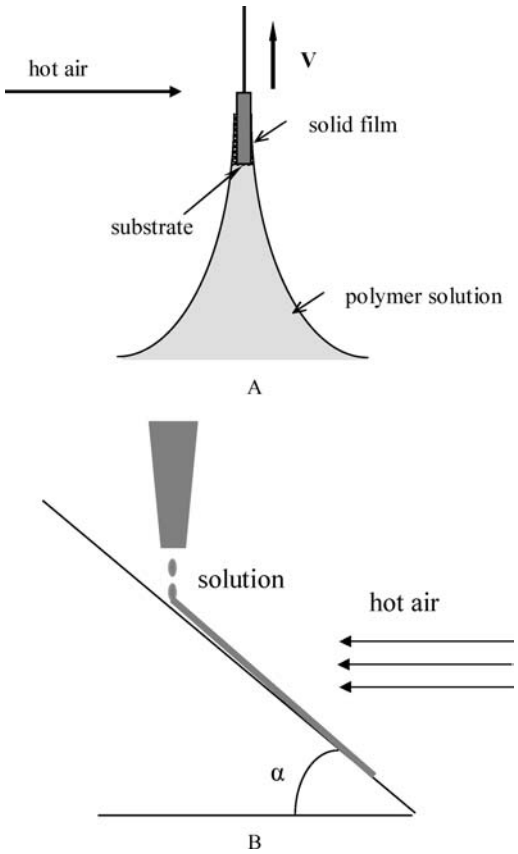

Figure 1 Schemes of the dip-coating deposition (A) and deposition on the tilted substrate (B).

When the substrate is dip-coated, the liquid film runs out from the polymer solution (which was kept under isothermic conditions: t_s = 5–30°C for chlorinated solvents and 20–110°C for aromatic solvents), adheres to the substrate surface and solidifies during the evaporation of the solvent (see Fig. 1A). Dip-coating was carried out with a high pulling speed V = 47 cm/min. Pulling direction was vertical in all our experiments. Films were immediately dried under different conditions: with a hot or room temperature air current parallel or normal to the substrate and in the closed box under isothermal conditions (t_d = 20°C). Gas current velocity ($v = 0.1 - 12$ m/s was measured with an anemometer (PROVA AVM 03). When the gas stream was normal to the substrate it was stabilized with a 0.5 m length tube. The drying temperatures were varied in the range $t_d = 20 - 100$°C.

When tilted substrates were coated, the same polymer solutions were dripped on the quartz glass substrates as depicted in Fig. 1B and dried with a hot air stream. The slope of the substrate was varied in the range $\alpha = 22–76°$. The structure of the dry film was studied by means of optical and scanning electron microscopy.

Pattern formation was visualized and studied *in situ* with a shadowgraph technique similar to those described by Weh and Kumacheva [3, 14].

3. Results and discussion

3.1. Optical microscopy and SEM study of the patterns: impact of the solvent and parameters of drying

When polymers were dissolved in aromatic solvents, transparent films with no patterning were obtained under all deposition techniques and all drying conditions. When films were dried slowly in the closed box homogenous transparent films without any patterning were obtained for all kinds of solvents and substrates.

Mesoscopic patterning was revealed with optical and SEM microscopy when substrates were coated with chlorinated solvent-based polymer solutions and were dried with the air stream. In this case, both deposition techniques (dip-coating and deposition on the tilted substrates) brought into existence very similar self-assembled, mesoscopically scaled patterns, depicted in Figs 2–5. There was no difference in the mesoscopic structure of the films obtained by dip-coating when hot air was blown in parallel and normally to the surface. It has been established that mesoscopic structuring takes place in both cases under broad ranges of drying temperatures (t_d = 20–100°C) and air stream current velocities (v = 0.1–12 m/s). In specific cases under high drying temperatures ($t_d > 60$°C) the mesoscopic oredering was destroyed, and the close-packed submicrometric patterns analogous to those reported previously by our group were observed [6].

The patterns are comprised of polymer domains separated by highly porous areas. Similar structures were reported by Weh and Shimomura [3–5], but the resemblance is superficial: in our case self-assembling takes

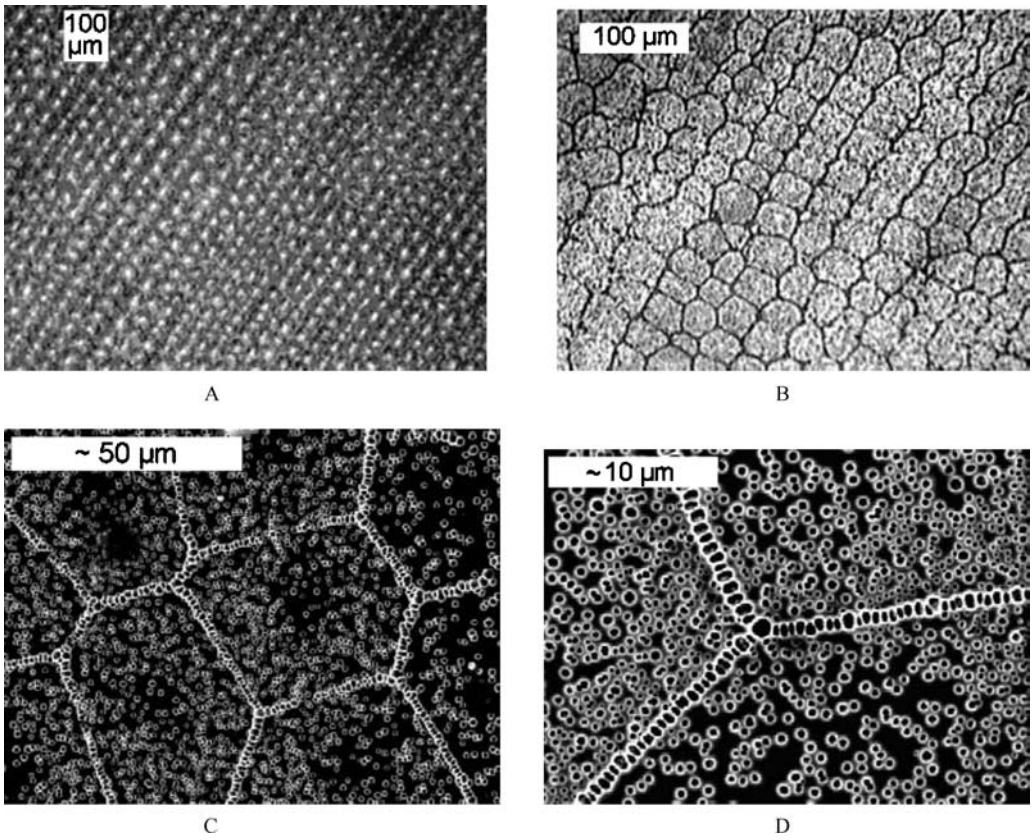

Figure 2 Optical microscopy and SEM images of self-organized mesoscopic structures obtained under fast dip-coating deposition of PMMA films on the quartz glass substrate. Solvent—dichloromethane. The drying temperature —90°C. A, B—Optical microscopy reveals ordered mesoscopic structure. C—SEM image of the mesoscopic cell. D—SEM image of the cell boundary.

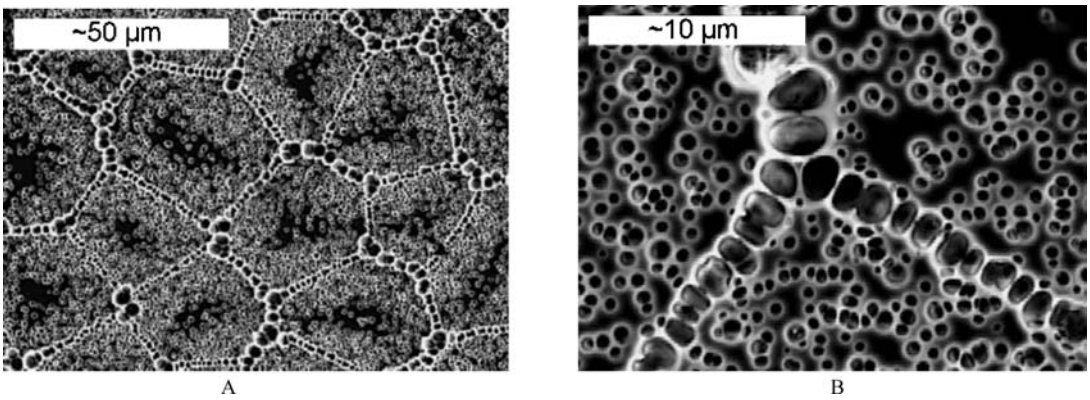

Figure 3 SEM images of mesoscopic patterns obtained under fast dip-coating deposition of PMMA film on the quartz glass substrate. Solvent—chloroform. The drying temperature –60°C. A—SEM image of mesoscopic cells. B—SEM image of the boundary.

place in the vertical or tilted flow of the evaporated solution. Pulling direction (vertical) and longitudinal direction of the structures depicted in Fig. 2 are identical. It is important to note that the characteristic size of the mesoscopic cell was 30–50 μm, and it was only slightly sensitive to the kind of polymer, substrate or deposition technique.

3.2. Shadowgraph visualization of the mesoscopic self-assembling

The shadowgraph technique allowed effective visualization of the mesoscopic self-assembling. Four distinct stages of the self-assembling process were observed. At the first stage thin ($\sim$1 μm thickness) boundaries are formed (Fig. 6A). Formation of these boundaries is inherent for chlorinated solvents only (distinctions between chlorinated and aromatic solvents will be discussed below).

This stage extends over the first 5 s of the drying process. Dimensions of the boundaries are very close to those of mesoscopic cells. We relate formation of these boundaries to polymer solution flow instability, the nature of which will be discussed below. At the second stage intensive boiling of the solvent begins (the low boiling point of

both solvents has to be emphasized). We have related already mesoscopic patterning to the boiling of the solvent [6, 7]; however, direct experimental verification of this hypothesis is reported first in the present paper. At this stage an intensive migration of the solvent vapor bubbles toward the cells boundaries has been observed (Fig. 6B). Similar lateral flow of the solvent due to the Marangoni surface tension instability was discussed previously by Weh [3]. At the third stage (Fig. 6C) the bubbles precipitate on the boundaries formed at the first stage of the drying process, thus yielding structures depicted in Fig. 2C and D. The characteristic time of these stages is of the order of 5 s. At the same stage a surprising phenomenon was revealed with shadowgraph technique: migration of the bubbles along the boundary toward network nodes (Fig. 6C) resulting in the formation of large nodal bubbles, displayed in Figs 3A,B and 5A. On the last stage (Fig. 6D) we observed intensive lateral migration of the bubbles, yielding the final structure of the mesoscopic cell. SEM images of these cells demonstrate that the central domain of the cell is much more free from pores than areas adjacent to the cell's boundary (Figs 3A and 4A), this phenomenon is due to the lateral motion of the bubbles. Porous domains of the mesoscopic cells are comprised of small pores with dimensions of 200–1000 nm, presented in Fig. 5B. Total time, necessary for the mesoscopic cell formation was estimated as 15 s.

3.3. Possible mechanisms responsible for the mesoscopic cell formation

At first glance, the phenomenon of mesoscopic self-assembling may be related to Marangoni surface tension instability, extensively studied both experimentally and theoretically [4, 14–22]. When films are dried by external air flow under low drying temperatures ($t_s > t_d$), conditions necessary for the formation of two-layer (gas phase/liquid) Marangoni instability are formed:

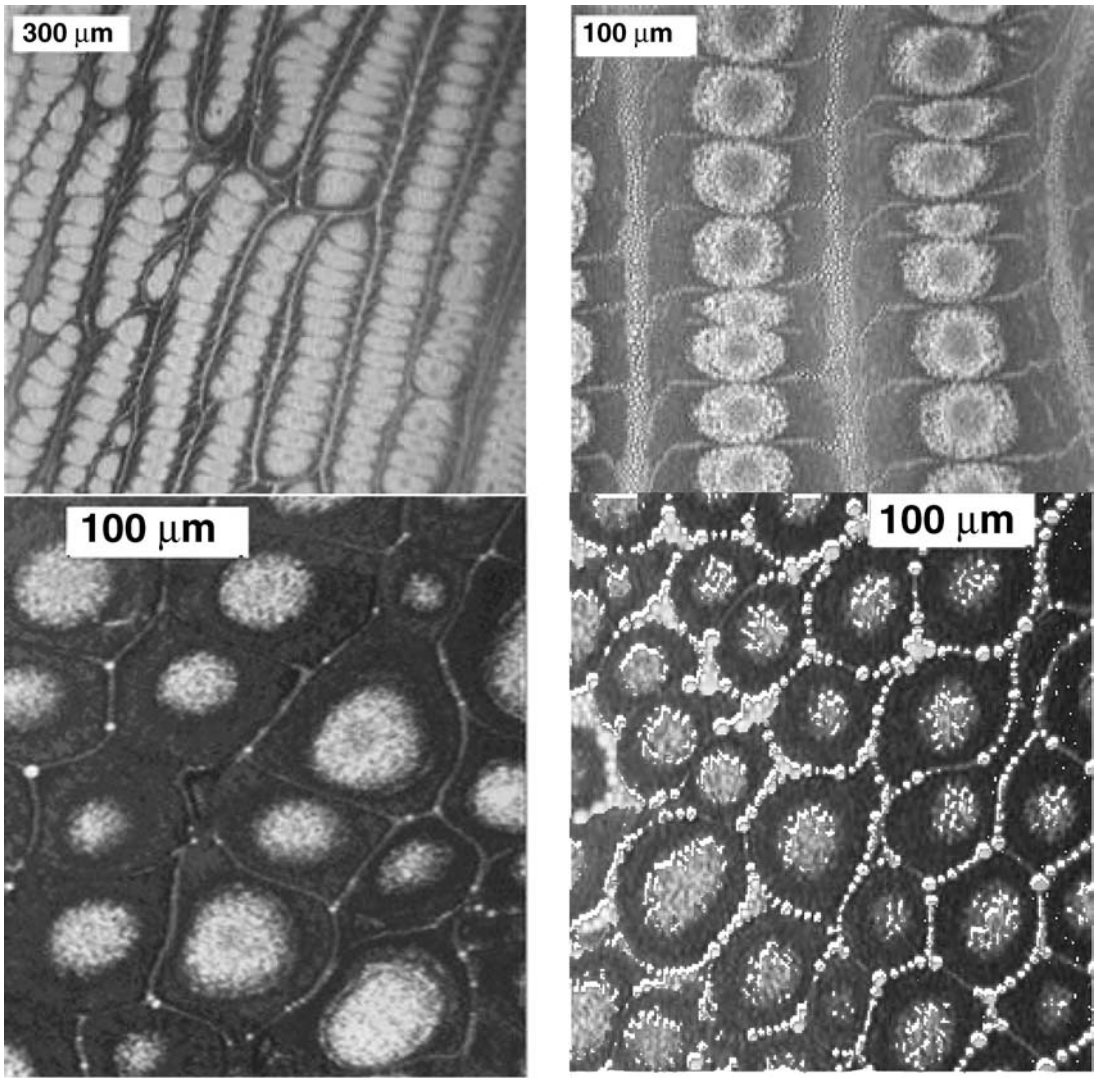

Figure 4 **A**. Optical microscopy images of self-organized mesoscopic PC films deposited on the tilted quartz glass substrate. Solvent - chloroform. The drying temperature −60°C. $\alpha = 76°$. **B**. SEM images of self-organized mesoscopic PC films deposited on the tilted quartz glass substrate. Solvent—chloroform. The drying temperature −60°C. $\alpha = 22°$.

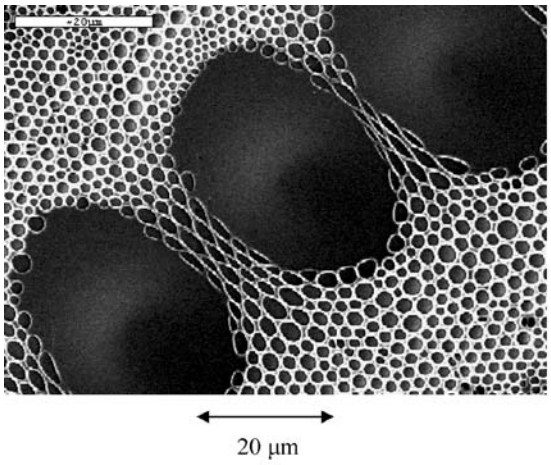

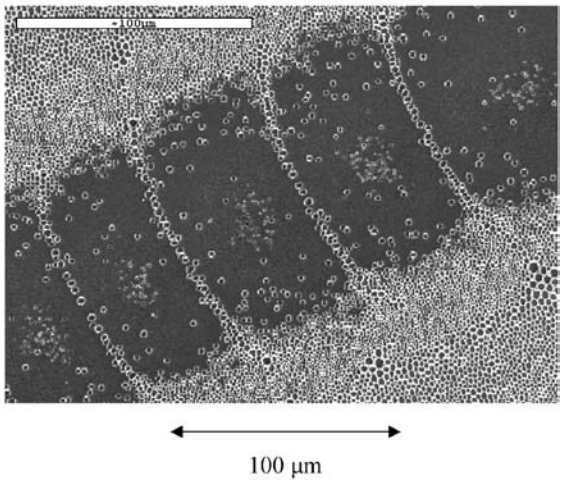

Figure 4 (Continued.).

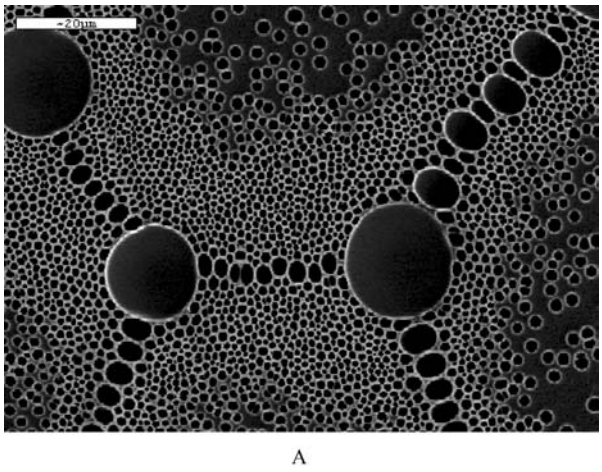

A

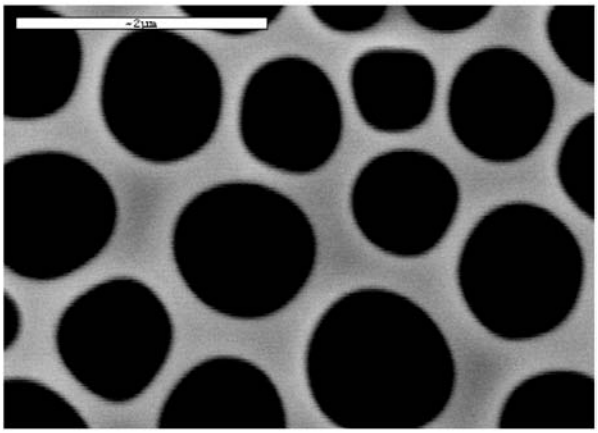

B

Figure 5 SEM images of self-organized mesoscopic PC films deposited on the tilted quartz glass substrate. Solvent—chloroform. The drying temperature -60°C. $\alpha = 76^{\circ}$. A—image of the area adjacent to the nodal points of the cell, B—image of the typical porous domain.

intensive cooling of thin liquid film with a sufficiently thin gas layer (due to both evaporation and blowing). The visual appearance of the network presented in Fig. 6A is very similar to patterns produced by Marangoni instability.

However, this phenomenon hardly explains some of the experimental facts: formation of mesoscopic cells under high drying temperatures $t_s < t_d$, whereas Golovin, Nepomnyashchy and Pismen established that "no monotonous instability occurs when the heating is from the gas phase" [21]. The second fact which has no explanation is the absence of mesoscopic cells when polymers were dissolved in aromatic solvents.

We already proposed another kind of mass transport instability, which is perhaps responsible for the mesoscopic cells formation [7]. De Gennes supposed that due to fast external drying, all solvent which leaves the solution is immediately removed from the system. Then, at an early stage of the evaporation process, a polymer–rich layer is formed [13]. According to earlier results, the characteristic thickness of such a layer may be on the order of 50–70 nm, about 20 times less than the characteristic thickness of the film by the end of drying. This boundary layer has an essentially lower diffusion coefficient than the bulk solution; therefore, the evaporation of the solvent is primarily governed by diffusion through this layer.

Now let us discuss the physical mechanism of diffusion instability: it is based on the observation that the local trough from outside the boundary layer has a tendency to grow as the reduced thickness facilitates the diffusion of the solvent in this place. Consequently, a local crest outside the boundary layer tends to grow as it suppresses the diffusion. Small–wavelength perturbations of this sort are suppressed by surface tension, and therefore there exists a critical scale for development of the layer instabilities. The critical wavenumber for stability was thus estimated as [7]:

$$k_{\text{crit}} \sim \sqrt[3]{\frac{(D\,\Delta c)^2 \rho}{s^4 \sigma}}$$

where D, ρ and σ are the diffusion coefficient, density and surface tension of the solution correspondingly, s is the boundary layer thickness and Δc is the dimensionless concentration jump at the boundary layer. For the sake of

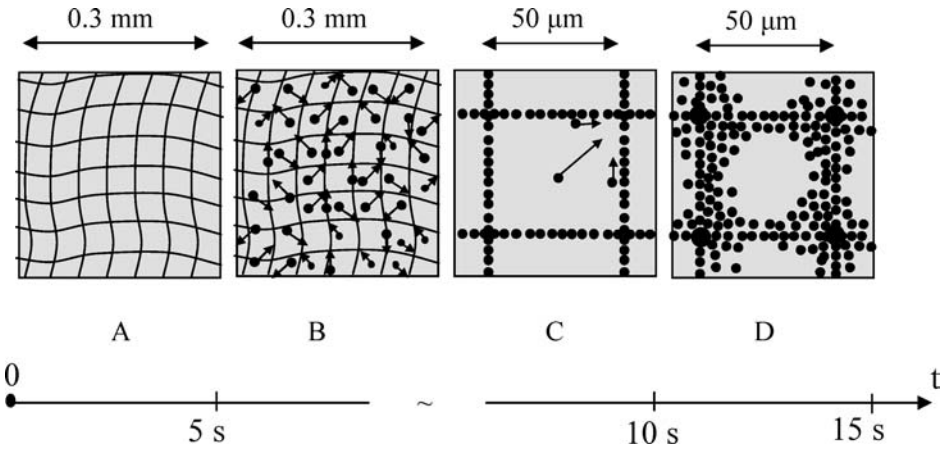

Figure 6 Main stages of the mesoscopic cell formation, revealed with shadowgraph technique: A—formation of the lateral "network", B—migration of solvent vapor bubbles to the network boundaries, C—migration of the bubbles along the cell's boundary, D—final formation of the mesoscopic cell.

numeric evaluation we take $s \sim 70$ nm (this estimation for the thickness of the boundary layer has been obtained by De Gennes in paper [13]) and the physical parameters of the solvents established experimentally [28–30]. Our estimation results on $k_{\text{crit}} \sim 6\times10^5$ m^{-1}. This estimation corresponds to the typical scale for the loss of stability equal to $2\pi/k_{\text{crit}} \sim 10$ μm. This figure qualitatively coincides with experimental findings. It could be seen that our estimation does not contain physical parameters of the polymer, but parameters of the solvent only, which are actually rather similar for different kinds of chlorinated solvents.

Our model supplies at least qualitative explanation for the fact that aromatic solvents do not produce mesoscopic patterns. Waggoner experimentally studied dependence of the chlorinated and aromatic solvent diffusion coefficient D on concentration in polystyrene solution [30]. He established that as polymer concentration increases chloroform data show a markedly steeper concentration dependence than does toluene. Solutions of PS in toluene a give linear dependence for the function $D(c)$, where c is a weight fraction of the polymer: $D = D_0 - kc$, (D_0 — is solvent self-diffusion coefficient) whereas the same dependence for polystyrene dissolved in chloroform fits well with $D = D_0(1 - c)^{\gamma}$, $\gamma = 1.6$.

This fact could explain why the use of chlorinated solvents brings into existence the phenomenon of mesoscopic patterning: fast changes in the diffusion coefficient favor formation of the local polymer-rich crests discussed above. However co-occurrence of traditional Marangoni instability and the instability discussed in the present paper is possible as well.

The subsequent stages of the mesoscopic cell formation connected with the bubbles migration are much more clear: what is actually seen in SEM and optical images is the frozen picture of the bubbles distribution. Higher drying temperatures favor formation of the thinner boundaries (see Figs 2–5).

4. Conclusions

Mesoscopic patterning in evaporated polymer films deposited on tilted and vertical substrates was studied. Polystyrene, polycarbonate and polymethylmethacrylate, when dissolved in chlorinated solvents, formed self-assembled mesoscopic structures, whereas the same polymers dissolved in aromatic solvents produced clear films. Shadowgraph visualization of the process demonstrated that at the first stage of the evaporation process a mesoscopic network was formed. Possible mechanisms of mesoscopic network formation were discussed. We supposed that diffusion instability could play a decisive role in this process. It was revealed by a shadowgraph technique that migration of the vapor bubbles toward the mesoscopic network plays the decisive role in the patterning process. Migration of the vapor bubbles along the network boundaries, resulting in the formation of large network nodes was observed as well.

Acknowledgements

The authors are grateful to Professor M. Zinigrad for his continuous support of our research activity. The authors are thankful to Professor A. Nepomnyashchy, Professor A. Voronel, Mr. A. Sheshnev for fruitful discussions. We thank Mrs. N. Litvak, Mr. Al. Shulzinger and Mrs. Maria Gorelik for SEM imaging of the samples. The work has been supported by the Israel Ministry of Absorption. O. V. Gendelman is grateful to the Taub and Shalom Foundations for their financial support.

References

1. D. GROSSO, F. CAGNOL, G. J. DE A. A. SOLER ILLIA, E. L. CREPALDI, H. AMENITSCH, A. BRUNET-BRUNEAU, A. BOURGEOIS and C. SANCHEZ, *Adv. Funct. Mater.* **14**(4) (2004) 309.
2. D. CHOWDHURY, A. PAUL and A. CHATTOPADHYAY, *J. Coll. Interf. Sci.* **265** (2003) 70.

3. L. WEH and A. VENTUR, *Macromol. Mater. Eng.* **289** (2004) 227.
4. L. WEH, *J. Coll. Interf. Sci.*, **235** (2001) 210.
5. O. KARTHAUS, L. GRASJO, N. MARUYAMA and M. SHIMOMURA, *Thin Solid Films*, **327–329** (1998) 829.
6. E. BORMASHENKO, R. POGREB, O. STANEVSKY, Y. BITON and Y. BORMASHENKO, *J. Mater. Sci.* **39** (2004) 639.
7. E. BORMASHENKO, R. POGREB, O. STANEVSKY, Y. BITON, Y. BORMASHENKO, T. STEIN, V. Z. GAISIN and R. COHEN, *Macromol. Mater. Eng.* **290** (2005) 114.
8. R. REIGADA, E. ABAD, J. CRUSATS, J. CLARET, J. IGNES-MULLOL and F. SAGUES, *J. Chem. Phys.* **121**(18) (2004) 9066.
9. T. NISHIKAVA, J. NISHIDA, R. OOKURA, S. I. NISHIMURA, S. WADA, T. KARINO and M. SHIMOMURA, *Mater. Sci. Eng. C* **10** (1999) 141.
10. W. P. LEE and A. F. ROUTH, *Langmuir* **20**(9) (2004) 9885.
11. X. MA, Y. XIA, E.-Q. CHEN, Y. MI, X. WANG and A.-C. SHI, *ibid.* **20**(22) (2004) 9520.
12. P. G. DE GENNES, *Eur. Phys. J. E* **6** (2001) 421.
13. Idem., *ibid.* **7** (2002) 31.
14. Z. MITOV and E. KUMACHEVA, *Phys. Rev. Letters* **81**(16) (1998) 3427.
15. M. LI, S. XU and E. KUMACHEVA, *Macromolecules* **33** (2000) 4972.
16. J. REICHENBACH and H. LINDE, *J. Coll. Interf. Sci.* **84** (1981) 433.
17. H. LINDE, M. G. VELARDE, W. WALDHELM and A. WIERSCHEM, *ibid.* **236** (2001) 214.
18. C. MOUSSY, G. LEBON and J. MARGERIT, *Eur. Phys. J. B* **40** (2004) 327.
19. P. PANIZZA, L. COURBIN, G. CRISTOBAL, J. ROUCH and T. NARAYANAN, *Physica A* **38** (2003) 322.
20. S. LIN-GIBSON, G. SCHMIDT, H. KIM, C. C. HAN and E. K. HOBBIE, *J. Chem. Phy.* **119**(15) (2003) 8080.
21. A. A. GOLOVIN, A. A. NEPOMNYASHCHY and L. M. PISMEN, *Physica D* **81** (1995) 117.
22. A. ORON, A. A. NEPOMNYASHCHY, *Phys. Rev. E* **69** (2004) 016313.
23. V. MITLIN, *J. Coll. Interf. Sci.*, **233** (2001) 153.
24. A. FRANK, *Eur. J. Mech. Fluids B* **22** (2003) 445.
25. S. NAIRE, R. J. BRAUN and S. A. SNOW, *J. Coll. Interf. Sci.* **230** (2000) 91.
26. R. BRUNISMA and Y. RABIN, *Phys. Rev. E* **49**(1) (1994) 554.
27. K. NAGAYAMA, *Coll. Surf. A* **109** (1996) 363.
28. F. X. PRIELMEIER and H.-D. LÜDEMANN, *Mol. Phys.* **58**(3) (1986) 593.
29. K. R. HARRIS, H. N. LAM, E. RAEDT, A. J. EASTEAL, W. E. PRICE and L. A. WOOLF, *ibid.* **71**(6) (1990) 1205.
30. R. A. WAGGONER, F. D. BLUM and J. M. D. MACELROY, *Macromolecules* **26** (1993) 6841.

Received 5 January
and accepted 17 May 2005